https://doi.org/10.5194/egusphere-2024-328
Preprint. Discussion started: 12 February 2024
© Author(s) 2024. CC BY 4.0 License.

Changes in South American Surface Ozone Trends: Exploring the Influences of Precursors and Extreme Events

Rodrigo J. Seguel [1, 2], Lucas Castillo [1, 2], Charlie Opazo [1, 2], Néstor Y. Rojas [3], Thiago Nogueira [4], María Cazorla [5], Mario Gavidia-Calderón [6], Laura Gallardo [1, 2], René Garreaud [1, 2], Tomás Carrasco-Escaff [1], Yasin Elshorbany [7]

[1]Center for Climate and Resilience Research (CR)[2], Santiago, Chile
[2]Department of Geophysics, Faculty of Physical and Mathematical Sciences, University of Chile, Santiago, Chile
[3]Department of Chemical and Environmental Engineering, Universidad Nacional de Colombia, Bogotá, Colombia
[4]Departamento de Saúde Ambiental, Faculdade de Saúde Pública, Universidade de São Paulo, São Paulo, Brazil
[5]Universidad San Francisco de Quito USFQ, Instituto de Investigaciones Atmosféricas, Quito, Ecuador
[6]Departamento de Ciências Atmosféricas, Instituto de Astronomia, Geofísica e Ciências Atmosféricas, Universidade de São Paulo, São Paulo, Brazil
[7]University of South Florida, St. Petersburg, USA

Correspondence to: Rodrigo J. Seguel (rodrigoseguel@uchile.cl)

Abstract

In this study, 21st-century ground-level ozone trends and its precursors in South America were examined, which is an understudied region where trend estimates have rarely been comprehensively addressed. Therefore, we provided an updated regional analysis based on validated surface observations. We tested the hypothesis that the recent increasing ozone trends, mostly in urban environments, resulted from intense wildfires driven by extreme meteorological events impacting cities where preexisting volatile organic compound (VOC)-limited regimes dominate. We applied the quantile regression method to estimate trends, quantify their uncertainties, and detect trend change points. Additionally, the maximum daily 8-hour average (MDA8) and peak-season metrics were used to assess present-day short- and long-term exposure levels (2017-2021). Our results showed lower levels in tropical cities (Bogotá and Quito), varying between 39 and 43 ppbv for short-term exposure and between 26 and 27 ppbv for long-term exposure. In contrast, ozone mixing ratios were higher in extratropical cities (Santiago and São Paulo), with a short-term exposure level of 61 ppbv and long-term exposure levels varying between 40 and 41 ppbv. Santiago (since 2017) and São Paulo (since 2008) exhibited positive trends of 0.6 and 0.3 ppbv yr^{-1}, respectively, with very high certainty. We attributed these upward trends, or no evidence of variation, such as in Bogotá and Quito, to a well-established VOC-limited regime. However, we attributed the greater increase in the extreme percentile trends ($\geq 90^{th}$) to heat waves and, in the case of southwestern South America, to wildfires associated with extreme meteorological events.

https://doi.org/10.5194/egusphere-2024-328
Preprint. Discussion started: 12 February 2024
© Author(s) 2024. CC BY 4.0 License.

1 Introduction

The global tropospheric ozone (O_3) burden has increased by 45% from 1850 to the present day due to anthropogenic precursor emissions (Szopa et al., 2021). Additionally, surface ozone has increased by 32-71% in the temperate and polar regions of the Northern Hemisphere relative to historical observations (1896-1975) (Tarasick et al., 2019). In contrast, the evidence of ozone changes in the Southern Hemisphere, including South America, is unclear and difficult to quantify due to the limited availability of ground-level monitoring stations (Tarasick et al., 2019; Fleming et al., 2018).

South America (10°N to 55°S) encompasses tropical, subtropical and midlatitude climates, in addition to high-altitude conditions within the Andes Mountain range (Garreaud et al., 2009). This continent also hosts essential ecosystems for global water and carbon cycles, including tropical and subtropical wetlands, Andean glaciers, the Amazon rainforest and peatlands in Patagonia (Gumbricht et al., 2017; Hoyos-Santillan et al., 2019; Heinrich et al., 2021; Lapere et al., 2023; Molina et al., 2015). In contrast, 85% of the continent's population, estimated at more than 430 million people in 2022, resides in urban areas (Population Reference Bureau 2024). In addition to geographical and climatological contexts, cities vary in terms of public transportation, industry, governance, regulation and the degree of clean energy penetration (Cazorla et al., 2022).

In South American countries, the enactment of air quality standards started in the 1990s and has progressively increased. Except for a few cities, air quality monitoring in the region provides records spanning no longer than one or two decades, contrasting with the spatial coverage and long-term records in other regions, such as North America and Europe (Schultz et al., 2017). Most countries set ozone standards ranging from 51 to 71 ppbv (Lyu et al., 2023). However, ozone regulation does not guarantee compliance, as observed in cities such as Santiago and São Paulo, which have been designated nonattainment areas for decades (Seguel et al., 2020; Andrade et al., 2017). Furthermore, photochemical pollution has generally received less attention than particle pollution despite the increasing role of photochemistry in secondary aerosol formation (Andrade et al., 2017; Menares et al., 2020).

In most urban areas with adequate monitoring coverage allowing characterization of the temporal and spatial variabilities in ground-level ozone, a chemical regime of ozone formation limited by volatile organic compounds (VOCs) has been established in previous work (Seguel et al., 2020; Silva et al., 2018; Silva Júnior et al., 2009). This chemical regime was also observed during COVID-19 pandemic lockdowns, when several cities experienced increased ambient ozone mixing ratios (e.g., Bogotá, Quito, Santiago, São Paulo and Lima) due to a decrease in nitric oxide (NO) emitted by motorized transportation vehicles (Seguel et al., 2022; Sokhi et al., 2021; Cazorla et al., 2021b).

Monitoring has also been implemented through the Global Atmospheric Watch (GAW) program at remote locations, which allows studying changes in the chemical composition at high altitude sites (e.g., Tololo and Chacaltaya at 2,200 and 5,500 m a.s.l., respectively) and at pristine locations such as Patagonia (Ushuaia) and Galapagos (Anet et al., 2017; Cazorla and Herrera, 2020). Background monitoring stations are essential for interpreting the feedback between the atmospheric composition and

https://doi.org/10.5194/egusphere-2024-328
Preprint. Discussion started: 12 February 2024
© Author(s) 2024. CC BY 4.0 License.

the intensification of extreme weather events as well as for studying changes in transport patterns that could favor stratosphere–troposphere exchange (STE) in the extratropics (Lu et al., 2019; Cooper et al., 2020).

In South America, temperature trends have increased, except along the west coast (Perú and Chile) (Gu and Adler, 2023; Falvey and Garreaud, 2009). The most significant warming has occurred in the tropics and central part of the continent. In contrast, opposite precipitation trends have been observed in different regions of South America. Notable drying has been found in central Chile and the southern part of the Amazon basin (Gu and Adler, 2023). Under this scenario, the combination of megadroughts (Garreaud et al., 2020), warmer summers and more frequent heat waves (Jacques-Coper et al., 2021; González-Reyes et al., 2023) provides favorable conditions for the onset of large-scale fires and subsequent emission of ozone precursors (Feron et al., 2023). However, the distribution of these air masses is complex and must be examined further, given the complexity of the topography and disruption of airflow by the Andes Mountain range. Moreover, the southern portions of South America are subject to long-range transport of ozone and its precursors, as demonstrated by the arrival of plumes derived from fires in 2019 and large amounts of biomass burning (Kloss et al., 2021; Daskalakis et al., 2022).

In this study, we examined the distribution and trends in ozone and its precursors in cities and background locations in South America and analyzed trend change points. We propose that the precursor ratio (nitrogen oxides to VOC) largely determines the observed ozone trends in South American urban environments, while short-lived but increasingly recurrent extreme weather events (high temperatures, low relative humidity levels and moderate to high winds) are the main drivers of the large positive ozone anomalies increasing the upper percentiles of ozone trends. By providing this updated regional analysis of the distributions and trends in ozone and its precursors, we contribute to a better understanding of trend changes within regional, hemispheric, and global contexts and identify information gaps to be resolved by the scientific community.

2 Methodology

Time series of surface-level ozone, nitrogen oxides (NO_x), carbon monoxide (CO) and meteorological variable data were obtained from governmental agencies in Bogotá, Colombia; Santiago, Chile; Quito, Ecuador; and São Paulo State, Brazil. These agencies follow their own data policies, including quality assurance/quality control procedures and traceability. Nonetheless, the authors assessed the datasets regarding quality flags, drift, completeness and representativeness to produce a homogenized dataset, which was utilized in this research and submitted to the TOAR-II database.

The 21st-century trend analyses described in Section 2.2 were performed individually for 74 air quality monitoring stations and 3 stations of the GAW program. Only 7 monitoring stations located in medium-sized cities (between ~50,000 and ~300,000 inhabitants), mainly in Chile, were included in this study due to the completeness of the data and lack of long-term time series. A similar situation occurred for some WMO stations and high-altitude sites, which did not pass the 75% filter of valid data.

https://doi.org/10.5194/egusphere-2024-328
Preprint. Discussion started: 12 February 2024
© Author(s) 2024. CC BY 4.0 License.

The time series retrieved from stations in the main cities were aggregated to provide the trend and uncertainty in the monitoring network of each city. Such aggregation and subdivision operations were performed according to local expert judgment, thereby accounting for representativity, altitude, topography and precursor sources.

We used CO data in the absence of systematic measurements of VOCs in South America to explore the ozone chemical formation regime. Since carbon monoxide is typically coemitted during fuel combustion and transport in urban environments, this pollutant can be used as a surrogate for anthropogenic VOCs. Our trend analysis did not explicitly provide the CO-to-NO_x ratio because the available time series exhibited different lengths and gaps. Therefore, we obtained CO, NO, (nitrogen dioxide (NO_2) and NO_x trends individually to infer the ozone formation regime, as well as their respective change points.

2.1 Short- and long-term ozone metric evaluation

Present-day short- and long-term ozone exposure levels were assessed, i.e., over 2017-2021, for all stations available. To evaluate short-term exposure, we utilized the 99th percentile of the annual distribution of the maximum daily 8-hour average (MDA8) mixing ratio. For long-term exposure, we used the peak-season value proposed by the World Health Organization (WHO, 2021), defined as the average MDA8 mixing ratio calculated for the six consecutive months of the year with the highest six-month running-average ozone mixing ratio. To identify sites at exposure risk, we used the MDA8 and peak-season guidelines, at 51 and 31 ppbv, respectively (WHO, 2021).

2.2 Trend analysis

We calculated daily and monthly means based on hourly data, ensuring 75% valid data each day and month. An anomaly was determined by calculating the difference between harmonic functions (6 and 12 months) and the observed monthly value.

Subsequently, we applied the quantile regression (QR) method to conduct trend analysis based on monthly anomalies following TOAR-II recommendations (Chang et al., 2023). We applied a moving block bootstrap algorithm to account for the autocorrelation and calculated standard errors of the trends. Trend uncertainty was expressed using a calibrated language based on the *p* value and signal-to-noise (SNR) ratio (i.e., trend/standard error) (**Table 1**). The adopted scale graduation aimed to communicate the trend reliability across TOAR-II Working Groups (WGs).

Table 1: Trend reliability scale according to TOAR-II recommendations (Chang et al., 2023).

***p* value**	**SNR value**	**Term**
$p \leq 0.01$	SNR ≥ 3	Very high certainty
$0.05 \geq p \geq 0.01$	$2 \leq$ SNR ≤ 3	High certainty
$0.10 \geq p \geq 0.05$	$1.65 \leq$ SNR ≤ 2	Medium certainty
$0.33 \geq p \geq 0.10$	$1 \leq$ SNR ≤ 1.65	Low certainty
$p \geq 0.33$	SNR < 1	Very low certainty or no evidence

https://doi.org/10.5194/egusphere-2024-328
Preprint. Discussion started: 12 February 2024
© Author(s) 2024. CC BY 4.0 License.

We used the piecewise linear trend method to detect change points in the time series (Muggeo, 2003). A detected change point was considered valid when the magnitude of the SNR values before and after the change point was maximized (≥ 2). We imposed a minimum period of 4 years after the occurrence of a change point to avoid detection at the extremes of the time series. The SNR used to detect change points was obtained from the piecewise linear trend (it is not the same SNR obtained from quantile regression).

We utilized the following linear regression model to calculate the trend in the entire time series:

$$y_t = \alpha + \beta t + \sum_{k}^{N} \gamma_k max\{t - x_{c_k}, 0\} + \varepsilon \tag{1}$$

where y_t is the monthly anomaly of the variable, t is the monthly index of the observed anomaly, α is a constant, and β is the linear trend before the first change point x_{c_1}. If any exists, x_{c_k} is the index of the change point, γ_k denotes the linear trend after each change point, with $k = 1, 2, \ldots, N$, N is the number of change points detected for each time series, and $max\{t - x_{c_k}, 0\}$ is equal to 1 for $t > x_{c_k}$ and 0 for $t \leq x_{c_k}$. When no change point is incorporated, the linear regression model is reduced to $y_t = \alpha + \beta t$. According to our linear regression model, the time series trend after the first change point is $\beta + \gamma_1$, and that after the second change point is $\beta + \gamma_1 + \gamma_2$. To calculate the standard error of the trend after a change point, the bootstrap algorithm is again applied over the time series segment. Finally, ε denotes the error of the linear regression.

3 Results and discussion

Major urban agglomerations are distributed in different latitudinal bands, altitudes and regions of South America, enabling regional interpretation despite the limited monitoring sites. Quito (0.12°S, 78.5°W, 2800 m a.s.l.) and Bogotá (4.6°N, 74.1°W, 2600 m a.s.l.) are located at high altitudes in the northwestern South American region within the tropical latitudinal band (defined between 20°N and 20°S). São Paulo (23.5°S, 70.5°W, 740 m a.s.l.) is located in southeastern South America within the subtropical band (defined between 20° and 30°S), and Santiago (33.5°S, 70.5°W, 500 m a.s.l.) is located in southwestern South America at the equatorward edge of the mid-latitude band (defined between 30° and 60°S).

3.1 Ozone distribution overview in urban environments: MDA8 and peak-season value

The MDA8 metric calculated for the present day (2017-2021) showed that the lowest short-term exposure levels were found in Bogotá (43 ppbv) and Quito (39 ppbv), both of which are located in the tropical band. In contrast, the highest levels of MDA8 were observed in Santiago (mid-latitude) and São Paulo (subtropics), at 61 ppbv. **Figure 1** shows the MDA8 value for each available air quality monitoring station, which indicates, in some cases, the main receptor sites in these urban agglomerations. Additionally, **Table 2** lists the aggregated stations in the subdivisions used to clearly interpret the data. In this

https://doi.org/10.5194/egusphere-2024-328
Preprint. Discussion started: 12 February 2024
© Author(s) 2024. CC BY 4.0 License.

regard, central and northern Bogotá, eastern Quito, northeastern Santiago (not shown in **Table 2** (77 ppbv)) and São Paulo Capital exhibited the highest MDA8 levels. Additionally, in São Paulo, the MDA8 metric was significantly lower at present than in the preceding five years.

Overall, the data suggested different spatial distributions of short- and long-term exposure to ozone within the cities considered in South America, as both metrics (MDA8 and peak-season value) were substantially lower in Quito and Bogotá than at the Santiago and São Paulo stations. This finding is not intuitive given the intense solar radiation at locations in the deep tropics that activates ozone photochemistry in the presence of urban emissions.

Table 2: MDA8 and peak-season metrics calculated from 2012-2016 and 2017-2021 (present day) with 95% confidence intervals and percentage changes in the urban agglomerations and subdivisions.

Subdivisions	MDA8 (ppb)			Peak season (ppb)		
	2012-2016	2017-2021	Change (%)	2012-2016	2017-2021	Change (%)
Bogotá	**42.2 [± 4.2]**	**42.8 [± 3.6]**	**1.4**	**24.9 [± 2.4]**	**26.4 [± 3.1]**	**+5.9**
Northern Bogotá	48.7 [± 1.2]	46.2 [± 3.8]	-5.0	27.5 [± 2.4]	27.6 [± 2.0]	+0.16
Central Bogotá	45.1 [± 6.1]	46.6 [± 7.3]	3.2	27.0 [± 3.2]	29.7 [± 6.4]	+9.7
Southwest Bogotá	35.6 [± 1.4]	38.2 [± 8.9]	7.3	22.0 [± 6.3]	25.2 [± 8.9]	+14
Southeast Bogotá	35.7 [± 4.8]	39.1 [± 1.5]	9.5	22.3 [± 6.9]	22.2 [± 1.5]	-0.52
Quito	**41.1 [± 1.7]**	**38.6 [± 1.9]**	**-6.0**	**26.3 [± 1.2]**	**26.7 [± 1.1]**	**+1.5**
Quito main urban area	40.0 [± 2.9]	36.9 [± 1.4]	-7.5	26.1 [± 1.3]	26.3 [± 2.0]	+1.1
Quito eastern valleys	42.2 [± 2.2]	41.5 [± 1.4]	-1.7	26.5 [± 3.9]	27.4 [± 1.5]	+3.5
Santiago	**61.2 [± 4.4]**	**60.7 [± 5.5]**	**-0.83**	**39.1 [± 2.6]**	**40.9 [± 2.9]**	**+4.5**
São Paulo (SPMA & SPC)	**76.6 [± 2.6]**	**61.3 [± 2.6]**	**-20**	**42.8 [± 1.9]**	**40.1 [± 1.7]**	**-6.1**
São Paulo Metropolitan Area (SPMA)	77.7 [± 5.4]	60.6 [± 3.4]	-22	42.3 [± 3.0]	38.5 [± 1.4]	-8.9
São Paulo Capital (SPC)	76.1 [± 3.0]	61.7 [± 3.6]	-19	43.0 [± 2.4]	40.9 [± 2.3]	-4.8
Coastal São Paulo	53.1 [± 5.2]	42.7 [± 4.9]	-20	29.0 [± 2.1]	28.4 [± 2.3]	-2.1
Industrial São Paulo	64.2 [± 5.8]	47 [± 13]	-27	29.3 [± 7.0]	28.9 [± 8.0]	-1.2
Inland São Paulo	64.4 [± 5.2]	57.9 [± 2.2]	-10	42.8 [± 1.7]	42.3 [± 1.7]	-1.2

Bogotá, Quito, Santiago, and São Paulo are busy urban centers where urban emissions comprise a significant source of ozone precursors. In these cities, a significant fraction of ozone precursors is emitted by vehicular fleets and has decreased according to air quality control measures such as the introduction of better fuel quality, sulfur content reduction, enforcement of three-way catalytic converters, stricter emission standards for new fleet vehicles and mandatory periodic technical inspection for in-use vehicles (Andrade et al., 2017; Nogueira et al., 2021; Osses et al., 2022). In addition to anthropogenic emissions, these cities exhibit particularities explaining the ozone and surface exposure levels reached, which are described below.

Ozone precursor transport changes seasonally on the Bogotá Plateau. Southeasterly winds dominate most of the day between April and September. These predominant winds are associated with relatively low ozone levels due to the presence of fewer upwind sources. From October to March, westerly winds in the afternoon hours are associated with the highest ozone levels

https://doi.org/10.5194/egusphere-2024-328
Preprint. Discussion started: 12 February 2024
© Author(s) 2024. CC BY 4.0 License.

and air quality standard exceedances (61 ppbv), especially in the northeast region of the city, which receives more photochemically processed air masses.

Bogotá and Quito are equatorial cities at high altitudes with plentiful solar radiation to favor high photochemical activity. Nevertheless, in Quito, ozone levels usually remain below the national air quality standard (51 ppbv), and short-term exposure levels are less than 40 ppbv (present day), as indicated earlier. Given the availability of urban precursors and sunlight, these relatively low ozone levels are counterintuitive. These ozone levels could be partially explained by intense vertical mixing, as detected in vertical profiles from routine ozone soundings in Quito (Cazorla et al., 2021a; Cazorla, 2017).

In the Santiago Basin, ozone precursor emissions in the city are typically transported toward the northeast during the afternoon hours, especially during the summer period (December-March), when a stronger valley-to-mountain breeze occurs. Santiago experiences a marked seasonal cycle that reaches a minimum ozone level in the winter months and a maximum in late summer, usually peaking in March when late summer high temperatures are combined with high postholiday vehicle activity. Thermally driven valley–mountain circulation results in the accumulation of ozone and ozone precursors aloft, which can increase surface ozone when a well-mixed boundary layer develops in the afternoon (Seguel et al., 2013; Lapere et al., 2021). Thus, the northeastern region of the city is characterized by the highest ozone standard exceedances.

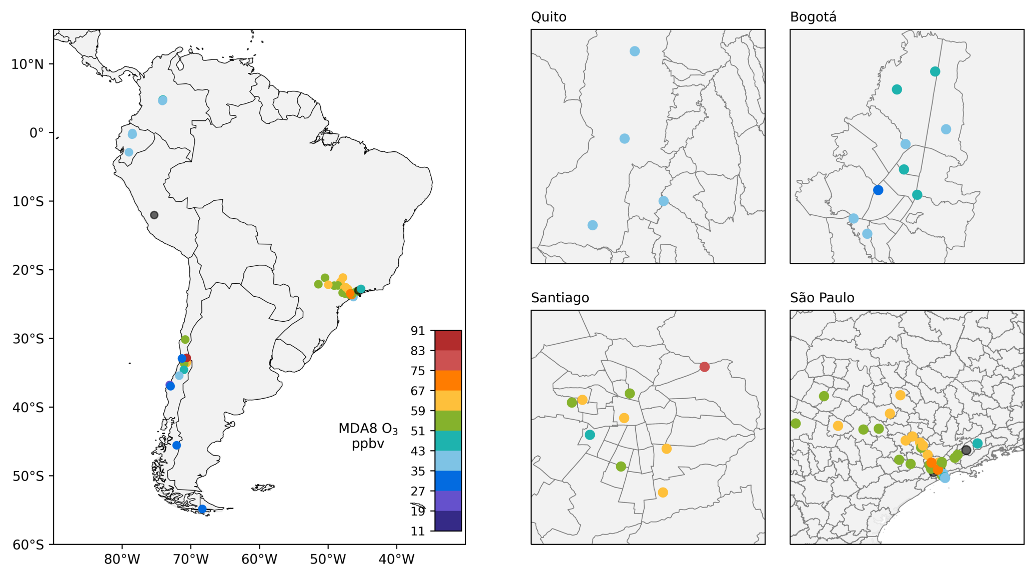

Figure 1: Present-day MDA8 ozone (2017-2021) in ppbv (nmol mol^{-1}) calculated from available South American monitoring stations (left panel). The right panels focus on Bogotá, Quito, Santiago and São Paulo. The black dots denote monitoring stations that do not meet the data quality criteria.

In the State of São Paulo, the main source of air pollution and ozone precursors is vehicular fleets, which widely use biofuels such as ethanol, gasohol (ethanol and gasoline mixture) and biodiesel (Andrade et al., 2017). High ozone mixing ratios are typically measured at the end of winter and in spring (late August to November), when clear sky conditions favor ozone

https://doi.org/10.5194/egusphere-2024-328
Preprint. Discussion started: 12 February 2024
© Author(s) 2024. CC BY 4.0 License.

formation (Carvalho et al., 2015). Additionally, in these months, biomass burning emissions from sugarcane burning occur in inland São Paulo, which can reach the São Paulo Metropolitan Area. As shown in **Figure 1**, high ozone mixing ratios can occur in inland São Paulo, caused by the transport of ozone precursors from the São Paulo Metropolitan Area under predominant southeasterly winds and inland biomass burning emissions (Squizzato et al., 2021).

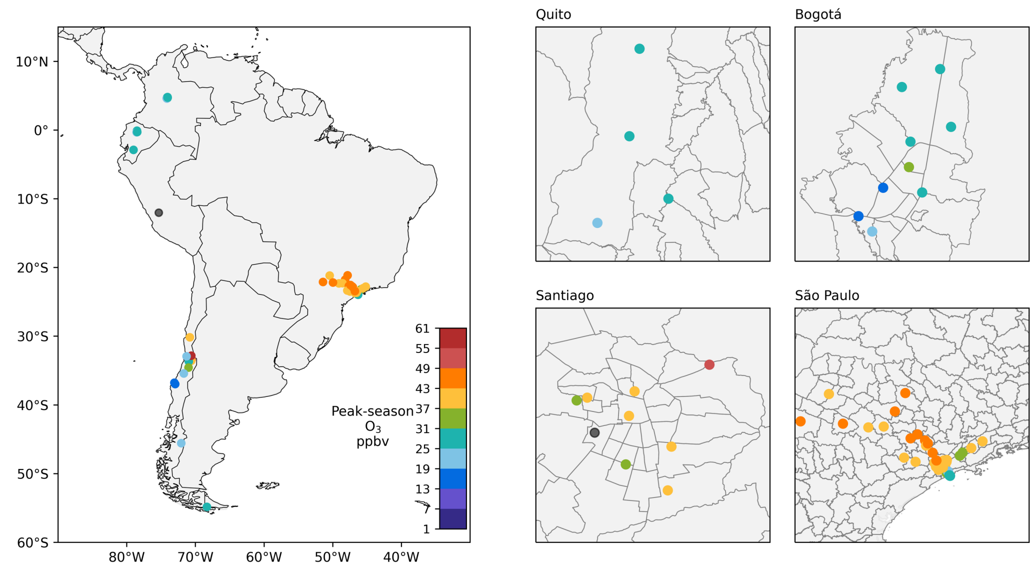

Figure 2: Peak-season ozone from 2017-2021 in ppbv (nmol mol^{-1}) calculated from available South American monitoring stations (left panel). The right panels focus on Bogotá, Quito, Santiago and São Paulo. The black dots denote the monitoring stations that do not meet the data quality criteria.

Mid-sized cities in South America, in contrast, face several challenges in terms of monitoring station availability and quality control. Notably, in Chile, out of 75 ozone monitoring stations, only 18 (9 located in Santiago) passed the quality control test established in the methodology, which is a warning in terms of the efficient use of resources.

Cuenca in Ecuador and southern Chilean mid-sized cities (<34° latitude) have low MDA8 levels. Coyhaique (45.6°S, 72.1°W, 356 m a.s.l.), located in southern Chile, which otherwise exhibits extremely high particle levels in winter due to wood burning, attains an MDA8 level of 27.3 ppbv. In contrast, Los Andes city in Chile (32.8 S, 70.6 W, 819 m altitude) exhibits the highest MDA8 level in South America (87.5 ppbv). Los Andes city has been described as a typical receptor site for air pollutants originating in the upwind Santiago Metropolitan Region (Seguel et al., 2013) and potentially from coastal areas, where high levels of VOCs have been measured in highly concentrated industrial zones (Seguel et al., 2023).

According to the long-term exposure metric, millions of inhabitants in Santiago and São Paulo are exposed to unhealthy ozone levels (**Figure 2**). Again, low peak-season levels were observed in Bogotá (26 ppbv) and Quito (27 ppbv). In contrast, peak-season exposure exceeded the 31 ppbv guideline in Santiago (41 ppbv) and in some São Paulo State subdivisions, such as São

https://doi.org/10.5194/egusphere-2024-328
Preprint. Discussion started: 12 February 2024
© Author(s) 2024. CC BY 4.0 License.

Paulo Capital, São Paulo Metropolitan Area and inland São Paulo (**Table 2**). Only coastal São Paulo and the industrial zone subdivisions occurred below the peak-season guideline.

In contrast to short-term exposure, which shows signs of improvement, mainly in São Paulo, present-day long-term exposure has led to more discrete improvements in São Paulo and increases in Bogotá, Quito and Santiago. Again, Los Andes city in Chile attained the highest peak-season value recorded (58 ppbv), followed by northeast Santiago (49 ppbv).

3.2 Ozone trends at urban and background sites

Ozone trends at the 50^{th} percentile and reliability are shown in **Figure 3**. The trend after the last detected change point (if any) is shown in **Figure 3**. Most change points detected in the time series occurred after 2010 (**Fig. A1 in Appendix A**). In addition, **Table 3** shows the extreme percentiles (5^{th} and 95^{th}) and the median trend in large cities. Regardless of the latitude of each large city analyzed, each urban agglomeration contains subdivisions with high-certainty positive ozone trends. The carbon monoxide trend is not clear (considering the calculated uncertainties) except for some subdivisions in São Paulo, where CO drastically declines. The Bogotá, Quito and Santiago stations showed an upward CO trend and a very low certainty (**Fig. S1 and S2**). The nitric oxide and nitrogen dioxide trends (with few exceptions) also trended downward (**Fig. S3-S8**). Both precursors are analyzed in more detail in the next section.

Three background monitoring stations are shown in **Figure 3**, including two high-altitude sites (Huancayo in Peru and Tololo in Chile), which are essential for studying the impact of stratosphere-to-troposphere transport on ground-level ozone. Huancayo (3310 m a.s.l., 12.04° S, 75.32° W) shows no evidence of increasing or decreasing ozone trends. The Tololo station, located in the subtropical Andean region (2220 m a.s.l., 30.17° S, 70.80° W), is one of the two WMO stations in South America with sufficiently long and complete time series to evaluate the impacts of both STE and poleward expansion of the Hadley circulation. At Tololo, an upward ozone trend of 0.29 ppbv $year^{-1}$ was observed between 2006 and 2014, with a very high certainty (**Table 3**). Notably, the trend change point in 2006 coincides with the global methane increase after the plateau observed between 1999 and 2006 (Lan et al., 2024). After 2014, although the trend was still positive (0.07 ppbv $year^{-1}$), the certainty was relatively low. The trend observed after 2014 was likely impacted by the COVID-19 pandemic in 2020 and possibly in 2021 (Putero et al., 2023). In contrast, Ushuaia, located in a net ozone depletion zone in the southernmost region of South America (Adame et al., 2019), showed a decreasing ozone trend, with a low rate (-0.07 ppbv $year^{-1}$) and high certainty (SNR>2.95). These trend estimations are consistent with previous work (Cooper et al., 2020).

https://doi.org/10.5194/egusphere-2024-328
Preprint. Discussion started: 12 February 2024
© Author(s) 2024. CC BY 4.0 License.

Table 3: Ozone trends and reliability estimated for large cities and Tololo station (5th, 50th (median) and 95th percentiles). The table also provides the time series period for each city, number of monitoring stations considered and year of the change point.

Location	Time series length	Stations	Percentile	Change Points	Piecewise dSNR	Trend (ppb year^{-1})	Confidence interval	SNR	p-value
Bogotá	Jan 2008 – Apr 2021	13	5th	Not detected	-----	0.03	0.25	0.21	$8.34 \cdot 10^{-1}$
			50th	Not detected		-0.02	0.19	-0.22	$8.26 \cdot 10^{-1}$
			95th	Not detected		-0.06	0.41	-0.3	$7.67 \cdot 10^{-1}$
Quito	Sep 2005 – Jan 2022	6	5th	Before Apr 2011	4.2	-0.3	0.33	-1.84	$6.67 \cdot 10^{-2}$
			5th	After Apr 2011		0.05	0.16	0.64	$5.65 \cdot 10^{-1}$
			50th	Before Apr 2011		-0.22	0.21	-2.14	$3.37 \cdot 10^{-2}$
			50th	After Apr 2011		0.06	0.14	0.9	$4.10 \cdot 10^{-1}$
			95th	Before Apr 2011		-0.63	0.75	-1.67	$9.57 \cdot 10^{-2}$
			95th	After Apr 2011		0.11	0.33	0.68	$3.22 \cdot 10^{-1}$
Santiago	Apr 1997 – Apr 2023	9	5th	Before Nov 2017	19	-0.20	0.07	-5.53	$6.70 \cdot 10^{-8}$
			5th	After Nov 2017		0.72	0.40	3.65	$4.60 \cdot 10^{-2}$
			50th	Before Nov 2017		-0.19	0.04	-8.78	$1.17 \cdot 10^{-16}$
			50th	After Nov 2017		0.62	0.44	2.79	$2.62 \cdot 10^{-3}$
			95th	Before Nov 2017		-0.26	0.08	-6.09	$3.32 \cdot 10^{-9}$
			95th	After Nov 2017		1.6	1.2	2.62	$1.43 \cdot 10^{-3}$
São Paulo	Jan 1998 – Dec 2020	21	5th	Before Mar 2008	6.1	-0.19	0.21	-1.8	$7.30 \cdot 10^{-2}$
			5th	After Mar 2008		0.38	0.27	2.81	$9.18 \cdot 10^{-3}$
			50th	Before Mar 2008		-0.17	0.23	-1.51	$1.33 \cdot 10^{-1}$
			50th	After Mar 2008		0.31	0.23	2.72	$3.81 \cdot 10^{-3}$
			95th	Before Mar 2008		-0.05	0.43	-0.25	$8.04 \cdot 10^{-1}$
			95th	After Mar 2008		0.43	0.32	2.68	$1.67 \cdot 10^{-2}$
Tololo	Dec 1995 – Dec 2021	1	5th	Before May 2006	3.6 / 4.2	-0.04	0.22	-037	$7.09 \cdot 10^{-1}$
			5th	2006 – 2014		0.16	0.16	1.98	$2.64 \cdot 10^{-4}$
			5th	After Apr 2014		0.33	0.48	1.37	$1.68 \cdot 10^{-1}$
			50th	Before May 2006		0.05	0.12	0.88	$3.82 \cdot 10^{-1}$
			50th	2006 – 2014		0.29	0.14	4.07	$2.41 \cdot 10^{-2}$
			50th	After Apr 2014		0.07	0.31	0.44	$7.39 \cdot 10^{-1}$
			95th	Before May 2006		-017	0.28	-1,17	$2.41 \cdot 10^{-1}$
			95th	2006 – 2014		0.40	0.19	4.16	$4.55 \cdot 10^{-2}$
			95th	After Apr 2014		0.04	0.29	0.29	$6.74 \cdot 10^{-1}$

https://doi.org/10.5194/egusphere-2024-328
Preprint. Discussion started: 12 February 2024
© Author(s) 2024. CC BY 4.0 License.

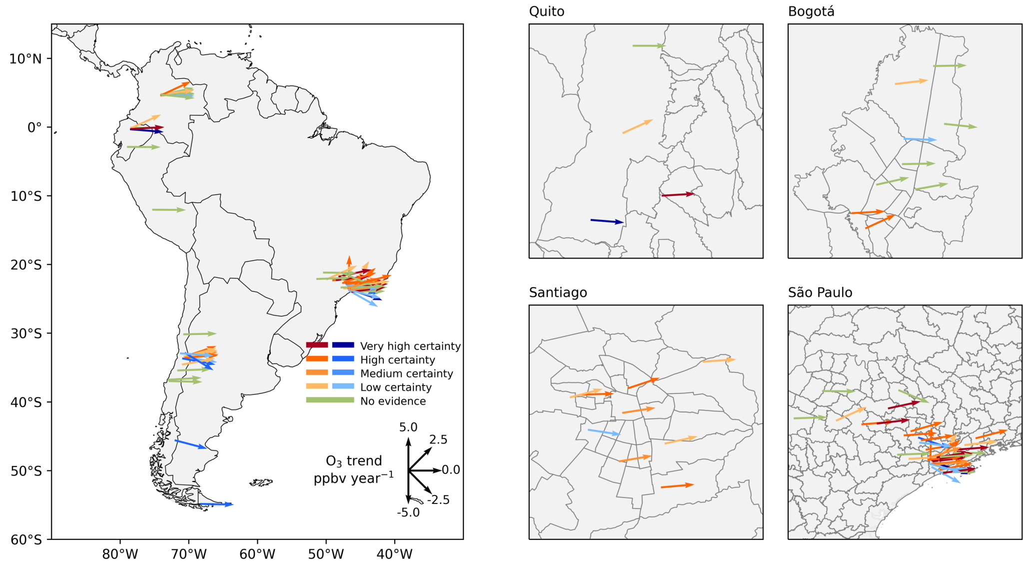

Figure 3: Ground-level ozone trends in ppbv year^{-1} and reliability levels calculated from available South American monitoring stations (left panel). When one or more change points are identified, the trend starts from the latest change point detected. The right panels focus on Bogotá, Quito, Santiago and São Paulo.

3.3 Ozone change points

Several South American urban agglomerations exhibit similarities in terms of implementing measures to reduce air pollution by limiting the accelerated growth in motorized vehicles. In general terms, we note that these ozone precursor abatement measures have been implemented, ignoring the VOC-to-NO_x ratio, suggesting that ozone increases once the VOC-limited regime is reached. The latter, together with the extensive wildfires around the cities studied, could explain the occurrence of trend change points at some sites.

The ozone mixing ratios in Bogotá showed no evidence of reduction or increase during the last decade despite efforts to reduce primary pollutant emissions, as shown in **Figure 4a**. However, in the northern area of the city, which is impacted by ozone formation in higher proportions, the median ozone trend decreased at a rate of -1.01ppb yr^{-1} (high certainty) between 2008 and 2013. After this period, there was a minor increasing trend (0.09 ppb yr^{-1}), with very low certainty.

Panels c and d in **Figure 4** show the trends in CO and NO_x in Bogotá to illustrate the ozone sensitivity to its precursors. CO showed a decreasing trend between 2008 and 2014 (-35 ppb yr^{-1} at the 50th percentile), attributable to improvements in the quality of fuels, renewal of vehicle fleets with better emission standards, and substitution of coal with natural gas at industrial facilities. From 2015 onwards, the trend changed to an increase in CO (3.6 ppb yr^{-1} at the 50th percentile), particularly in the high percentiles (>45th). This could be explained by the increase in the motorcycle fleet of the city, whose emission standard is lower than that of passenger cars (Rojas et al., 2023). In contrast, despite showing a change point in 2013, the NO_x mixing

https://doi.org/10.5194/egusphere-2024-328
Preprint. Discussion started: 12 February 2024
© Author(s) 2024. CC BY 4.0 License.

ratio continued to decrease, although at a lower rate. NO_x decreased rapidly between 2008 and 2012 (-3.9 ppb yr^{-1} at the 50th percentile) and more slowly after 2013 (-0.84 ppb yr^{-1} at the 50th percentile).

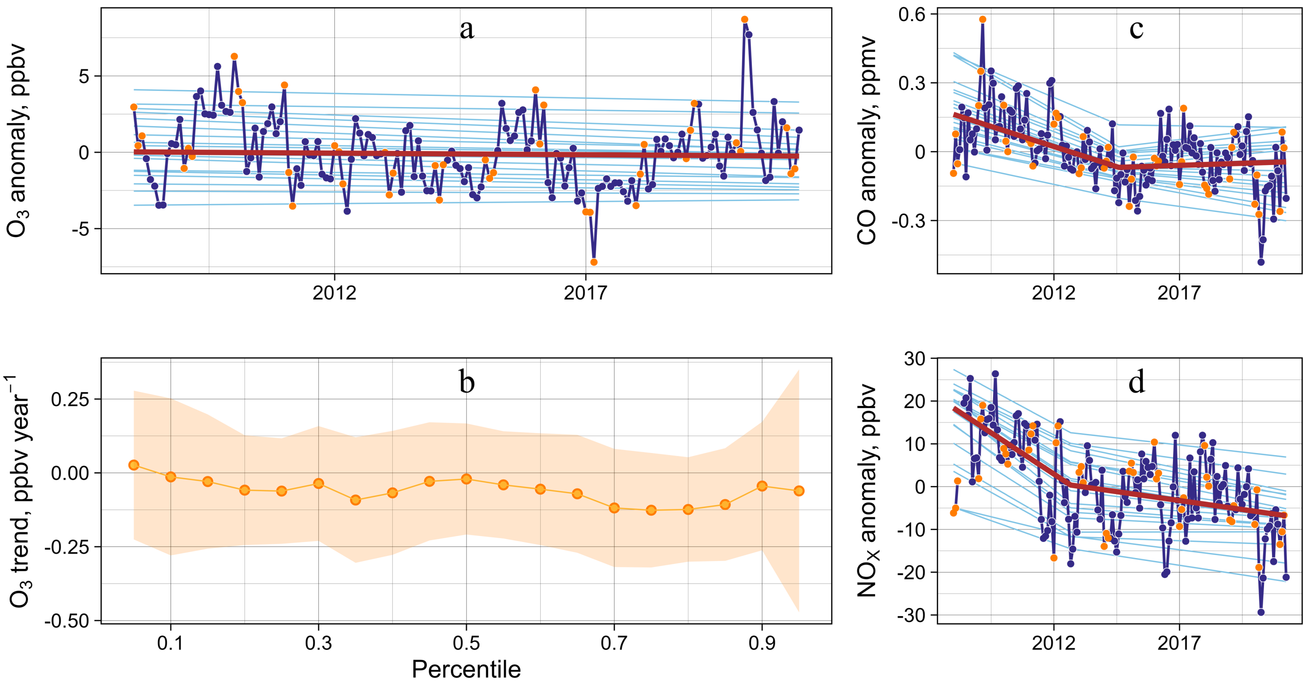

Figure 4: Percentile trends derived by quantile regression based on the monthly surface ozone (Panel a), carbon monoxide (Panel c) and nitrogen oxides anomalies (Panel d) in Bogotá. The orange dots in Panels a, c and d indicate the first three months of every year for reference purposes. In Panels a, c and d, the red line corresponds to the 50th percentile, and the light blue lines correspond to the remaining percentiles. Panel b shows the percentile trends of quantile regression from the 5th to 95th percentiles at 5 percentile intervals in Bogotá.

In Quito, the median ozone trends slowly decreased until March 2011, at a rate of -0.22 ppbv yr^{-1} (high certainty). After the change point, the trend reliability was very low. Therefore, there was no evidence of a change in the ozone trend (**Figure 5a**). After the change point, the segment was accompanied by a negative trend in NO of approximately -0.96 ppbv yr^{-1}. Overall, in the Quito NO_x-saturated environment, decreases in NO_x precursors were anticorrelated with increases in ozone.

Furthermore, starting in 2010, efforts to improve mobility in cities whose traffic was increasingly difficult to manage caused city authorities to adopt mobility restrictions by plate number during the morning and evening rush hours. The implementation of this policy probably shifted the composition and proportion of precursors, especially during the morning. This change generally coincided with the time series period when the ozone trend stopped decreasing, leading to a change point (**Figure 5a**).

https://doi.org/10.5194/egusphere-2024-328
Preprint. Discussion started: 12 February 2024
© Author(s) 2024. CC BY 4.0 License.

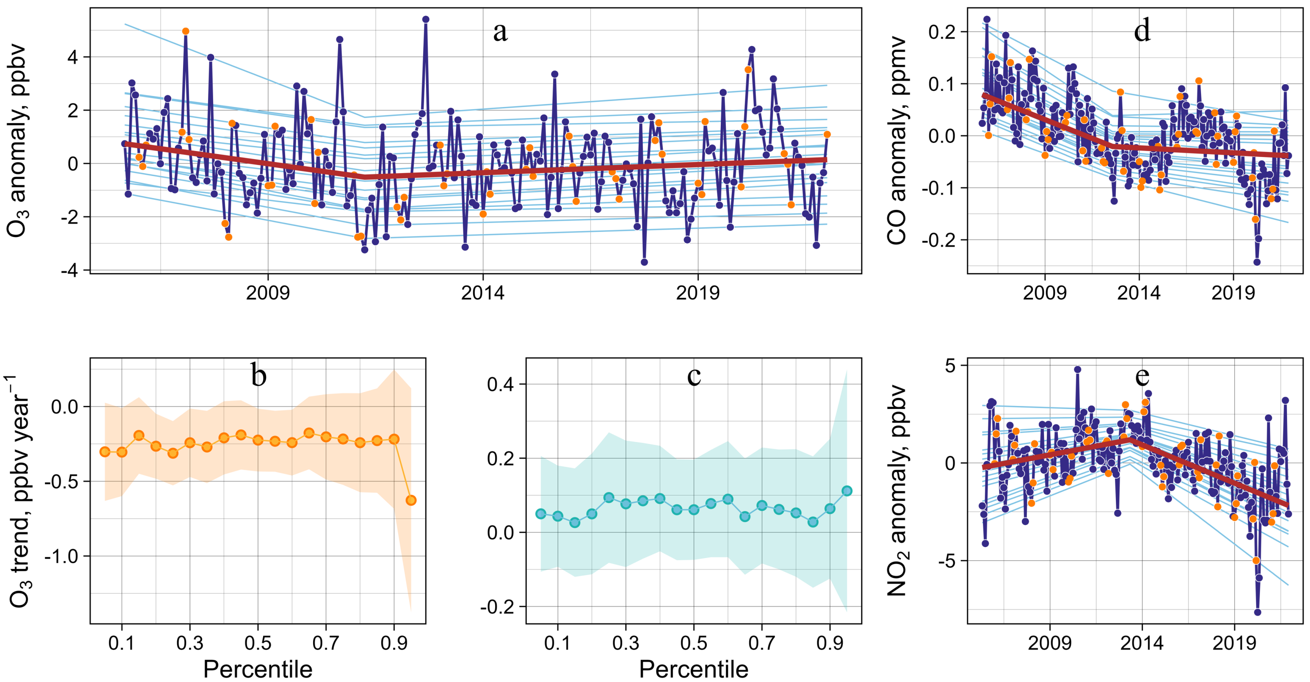

Figure 5: Percentile trends derived by quantile regression based on the monthly surface ozone (Panel a), carbon monoxide (Panel d) and nitrogen dioxide anomalies (Panel e) in Quito. The orange dots in Panels a, d and e indicate the first three months of every year for reference purposes. In Panels a, c and d, the red line corresponds to the 50th percentile, and the light blue lines correspond to the remaining percentiles. Panels b and c show the percentile trends of quantile regression from the 5th to 95th percentiles at 5 percentile intervals before and after the change point in Quito.

Ozone in Santiago decreased for nearly two decades due to public policies focusing mainly on curbing particulate matter. **Figure 6a** shows the percentile trend based on monthly ozone anomalies for the entire city of Santiago. The median trend showed that between 1997 and 2017, ozone decreased at a rate of -0.19 ppb yr^{-1} (very high certainty). After December 2017, an increase of 0.62 ppbv yr^{-1} was observed for the last five years (very high certainty). **Figure 6b** and **6c** shows the percentile trends before and after the change points. Up to 2017, the highest percentiles (≥80th) exhibited the most significant decreasing trends (> -0.23 ppbv yr^{-1}). In contrast, after the 2017 change point, the highest percentiles (≥80th) showed greater increasing trends (>0.91 ppbv yr^{-1}). In other words, until 2017, the policies effectively lowered the highest ozone percentiles.

https://doi.org/10.5194/egusphere-2024-328
Preprint. Discussion started: 12 February 2024
© Author(s) 2024. CC BY 4.0 License.

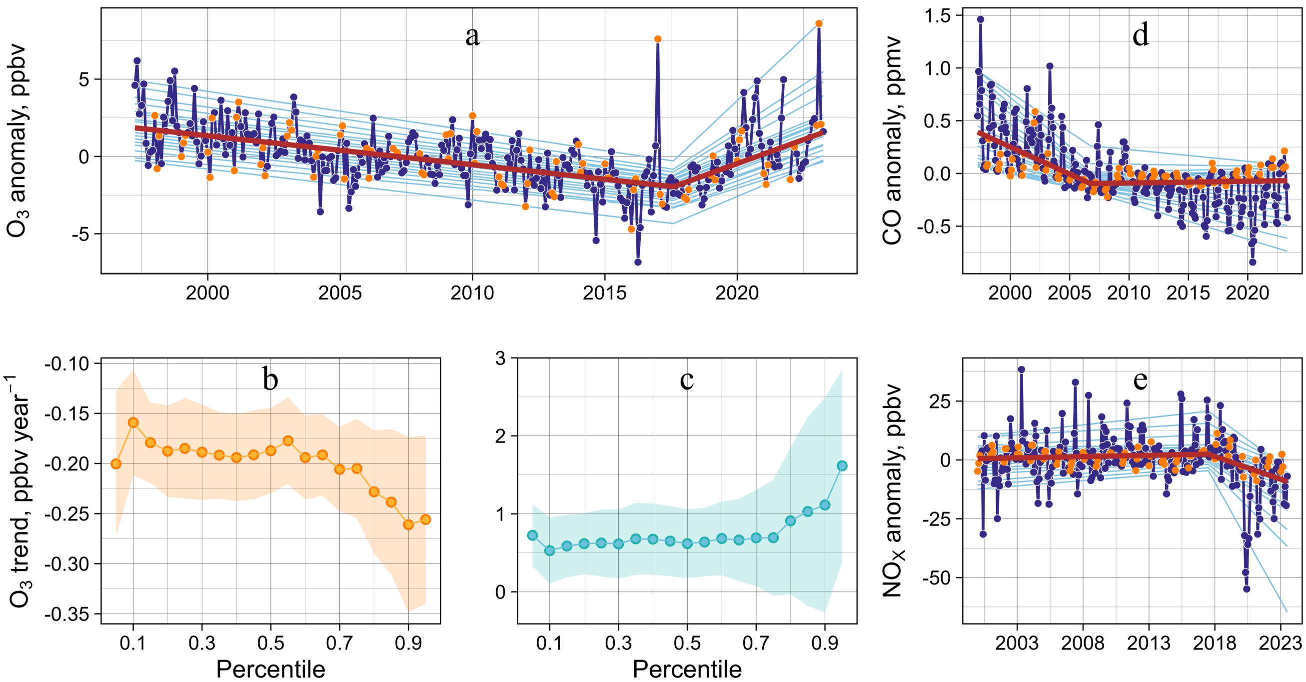

Figure 6: Percentile trends derived by quantile regression based on monthly surface ozone (Panel a), carbon monoxide (Panel d) and nitrogen oxides anomalies (Panel e) in Santiago. The orange dots in Panels a, d and e indicate the first three months of every year for reference purposes. In Panels a, d and e, the red line corresponds to the 50th percentile, and the light blue lines correspond to the remaining percentiles. Panels b and c show the percentile trends of quantile regression from the 5th to 95th percentiles at 5 percentile intervals in Santiago before and after the change point.

Ozone sensitivity to NO_x and CO is observed in **Figure 6**. The carbon monoxide anomalies clearly improved after 2010, resulting from the massive introduction of natural gas in the Santiago Metropolitan Region in 2009 (Mena-Carrasco et al., 2012). Notably, the cold month anomalies (April-September) decreased drastically. However, the warm month anomalies (October-March) started to increase again after 2017. In turn, the median trend remained flat after 2006. In contrast, the nitrogen oxide mixing ratio decreased after 2017 (-1.94 ppb yr^{-1}). Thus, the CO-to-NO_x ratio provides a favorable scenario for efficient ozone formation.

Over the last two decades, NO_x and CO mixing ratios have successfully decreased in the São Paulo Metropolitan Area, despite the growth in the vehicular fleet, due to regulations aimed at abating motorized vehicle emissions (**Figure 7**). The Brazilian Program for the Control of Air Pollution Emissions of Motor Vehicles has contributed to decreasing vehicular emissions in Brazil. In this regard, reductions in CO and NO_x emissions from light- and heavy-duty vehicles varying between -2.9% and -5.1% per year between 2001 and 2018 have been accomplished (Nogueira et al., 2021). These measurements have been accompanied by an increase in ozone since 2008. A similar trend was shown by Andrade (2017), where an increase in ozone mixing ratios was found after 2006, which coincides with previous reports analyzing data until 2017 (Pérez-Martínez et al., 2015; Carvalho et al., 2015; Schuch et al., 2019).

https://doi.org/10.5194/egusphere-2024-328
Preprint. Discussion started: 12 February 2024
© Author(s) 2024. CC BY 4.0 License.

Notably, many higher anomalies occurred in the warmer months (Jan-Feb) and were more frequent after the ozone change point in 2008 (**Figure 7a**). As a result, the ozone trends at the 90th and 95th percentiles increased at rates of 0.44 and 0.43 ppb yr^{-1}, respectively, compared with those in the lower 80th-15th percentiles (**Figure 7c**).

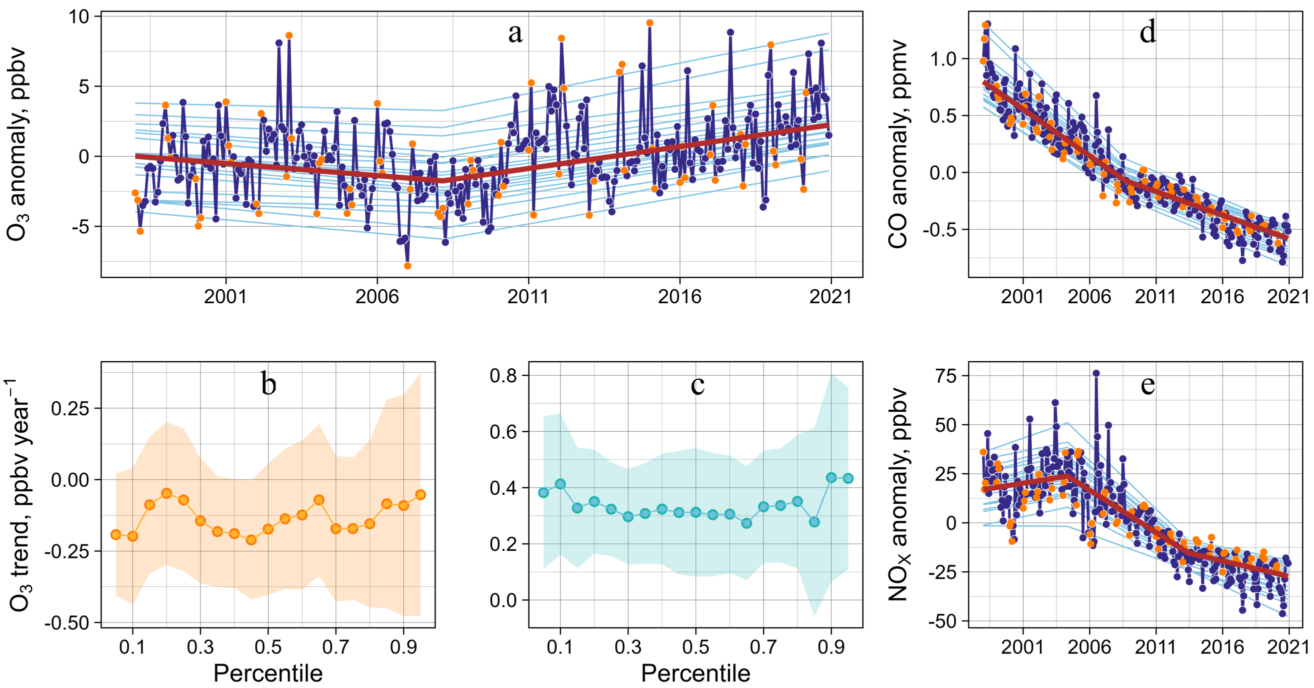

Figure 7: Percentile trends derived by quantile regression based on the monthly surface ozone (Panel a), carbon monoxide (Panel d) and nitrogen oxides anomalies (Panel e) in São Paulo. The orange dots in Panels a, d and e indicate the first three months of every year for reference purposes. In Panels a, d and e, the red line corresponds to the 50th percentile, and the light blue lines correspond to the remaining percentiles. Panels b and c show the percentile trends of quantile regression from the 5th to 95th percentiles at 5 percentile intervals in São Paulo before and after the change point.

3.4 Extreme ozone anomalies

As has been widely characterized in the literature, ozone anomalies and their precursors clearly show the effect of pandemic confinement in 2020 in many South American cities. In Santiago, positive ozone anomalies occurred in April (4.1 ppbv) and October (4.9 ppbv) 2020; in Quito in March (3.5 ppbv), April (4.3 ppbv) and October (3.2 ppbv); and in São Paulo in April (7.3 ppbv) and September (8.1 ppbv).

In turn, in Bogotá, the emission reductions during the COVID-19 lockdowns, combined with the transport of precursors emitted during biomass fires in the Colombian-Venezuelan plains (Ballesteros-González et al., 2020), contributed to positive extreme ozone anomalies in March (8.7 ppbv) and April (7.7 ppbv) (Sokhi et al., 2021; Mendez-Espinosa et al., 2019). During this event, the highest ozone mixing ratios were associated with clear skies, notable thermal inversion, stagnant conditions, and westerly winds in the afternoon, which trapped the air against the eastern mountains that border the city.

https://doi.org/10.5194/egusphere-2024-328
Preprint. Discussion started: 12 February 2024
© Author(s) 2024. CC BY 4.0 License.

Also, the long-lasting drought that has affected the west coast of subtropical South America, coupled with extreme weather configurations, has resulted in conditions capable of modifying the fire regime in southern-central Chile (mid-latitudes) (González et al., 2018). The meteorological pattern includes extreme temperatures (not necessarily heat waves) and low relative humidity levels with a high-pressure system that provides atmospheric stability, i.e., descending air masses and warm and dry wind, which cause fire propagation. In this regard, extreme positive ozone anomalies were observed in January 2017 (7.6 ppb) and February 2023 (8.6 ppb), caused by ozone and precursors transported from areas affected by intense wildfires (**Fig 6a**). **Figure B1** (**Appendix B**) shows events in early February 2023 characterized by many active fires whose impact was quantifiable by satellite observations. During this period, high CO (1.23 ppmv) and MDA8 ozone levels (117 ppbv) were observed in Santiago and locations to the south in early February. In contrast, the increase in nitrogen oxides was less than that observed for CO and O_3, which may be due to the rapid conversion of nitrogen oxides into other more oxidized forms, such as particulate nitrate, during plume transport (Juncosa Calahorrano et al., 2021).

In Quito, warmer summers, whose maximum values are typically reached between August and September, together with the occurrence of wildfires in the surrounding woods of the city, have also produced high ozone mixing ratios. Although not all these events were sufficiently extended in time to produce significantly high monthly anomalies, the September 2015 anomaly coinciding with a fire is notable, as shown in **Figure 5a**.

In the case of São Paulo, biomass burning is typically greater in September. This period marks the end of the dry season, when most air masses move from the northern and central-western regions of Brazil toward the south (São Paulo). However, with few exceptions, September is not the month with the highest anomalies. Indeed, many of the extreme ozone anomalies observed after the trend change point occurred in months in which long heat waves have been reported (Valverde and Rosa, 2023): February 2012 (11 days), October 2014 (10 days), January 2015 (13 days) and January 2019 (**Fig. 5a**).

Conclusions

Short-term (MDA8) and long-term (peak-season) exposure metrics calculated for the present day (2017-2021) revealed latitudinal differences in South America. The tropical cities of Bogotá and Quito attained lower ozone exposure levels than the large extratropical cities of Santiago in Chile and São Paulo in Brazil. Factors such as convection and vertical mixing within a convective tropical setting could explain, in part, the lower levels of ozone observed in Quito and Bogotá. Medium-sized cities located downwind of Santiago and São Paulo also showed high ozone exposure levels.

Santiago and São Paulo contained receptor sites and urban subdivisions with positive trends and high certainty after the detected change points (mainly after 2010). Quito (after a change point) and Bogotá showed no evidence of variations in ozone trends. We attributed these observed ozone trends to a greater decrease in nitrogen oxides than in carbon monoxide, which resulted in the establishment of volatile organic compound-limited regimes.

https://doi.org/10.5194/egusphere-2024-328
Preprint. Discussion started: 12 February 2024
© Author(s) 2024. CC BY 4.0 License.

The relatively greater reduction in nitrogen oxides during the COVID-19 pandemic (mostly limited to 2020) combined with warmer summers and intense wildfires in the region produced extreme positive ozone anomalies capable of increasing the highest percentiles. The 95th percentile trends in Santiago and São Paulo were 1.6 and 0.43 ppbv year^{-1} over 6 and 15 years, respectively. Therefore, extreme positive ozone anomalies in large urban agglomerations, whose ozone production regime is mostly VOC limited, constitute a regional challenge regarding ozone precursor mitigation and adaptation to warmer temperatures and new fire regimes.

Tololo is a valuable background site on the west coast of subtropical South America that showed signs of increased ozone. The ozone increase observed between 2006 and 2014 is notable, which, from a broader perspective, warns regarding changes in the ozone baseline.

These results advance the current knowledge described in the literature that addresses ozone trends in South America, which roughly provides surface ozone trends but overlooks change point attribution. However, the drawbacks of this study include the large unmonitored areas in the region and the lack of quality control, which prevents the inclusion of additional existing measurements. Additionally, the absence of systematic monitoring of volatile organic compounds makes it difficult to determine the contributions of anthropogenic and biogenic reactive species to ozone trends.

Finally, our results revealed signs of a climate penalty for ozone in South America and identified extratropical zones as those where the increase in ozone poses the highest risk. These observation-based results provide new evidence for comparison with trends in the free troposphere based on reanalysis, satellite observation, and numerical simulation data.

https://doi.org/10.5194/egusphere-2024-328
Preprint. Discussion started: 12 February 2024
© Author(s) 2024. CC BY 4.0 License.

Appendix A: Year of the last detected ozone trend change point

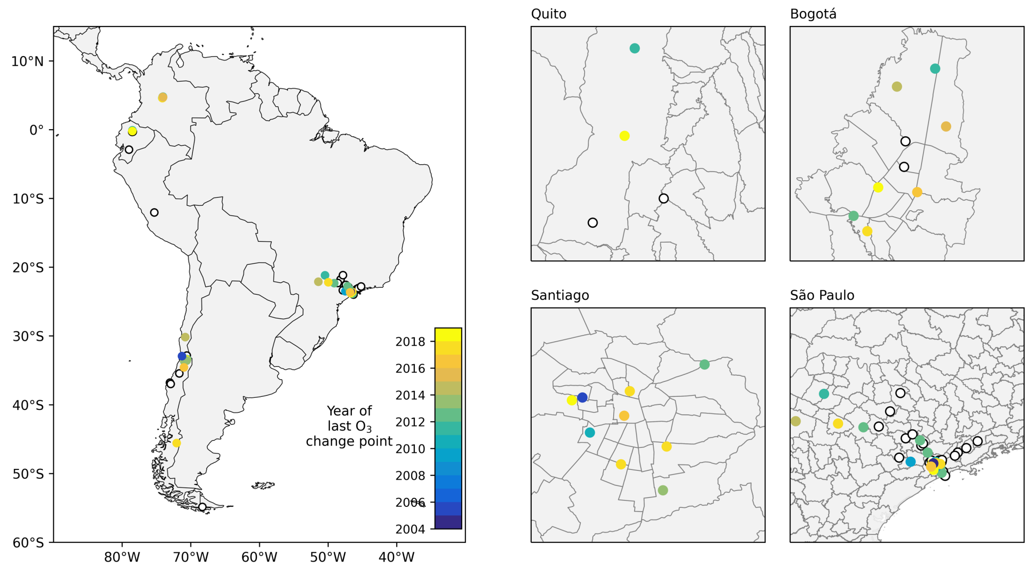

Figure A1: Year of the last detected ozone trend change point in South American monitoring stations (left panel). The right Panels focus on Bogotá, Quito, Santiago and São Paulo. The white dots denote stations with no change point detected.

Appendix B: Ozone and ozone precursors time series during 2023 wildfires in central Chile

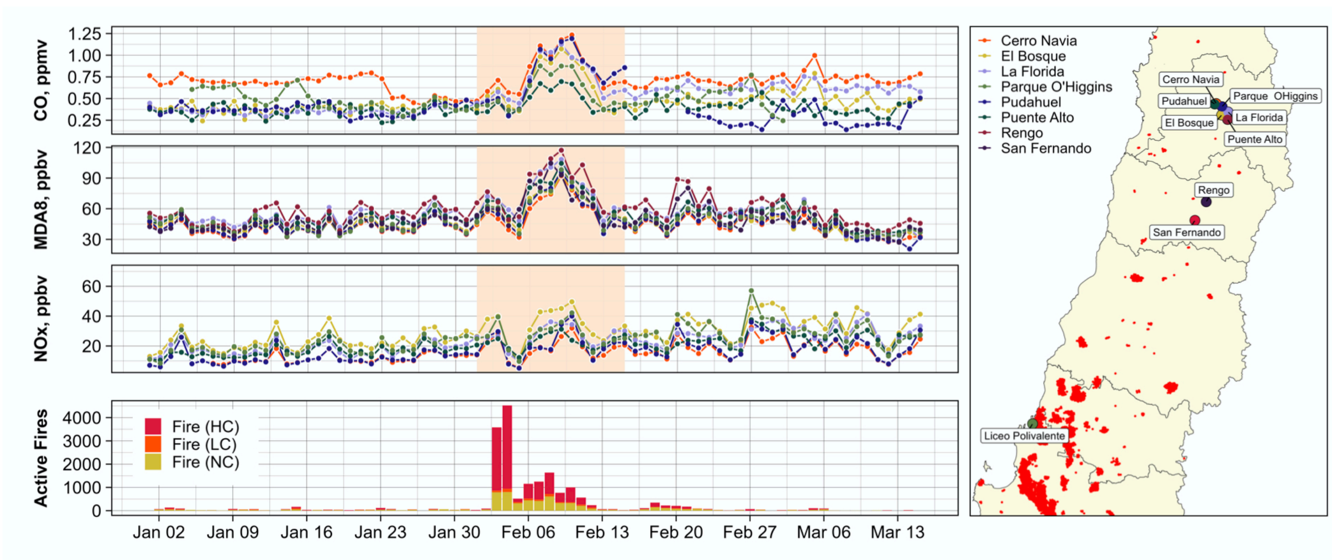

Figure B1: Time series of the maximum daily 8-hour average (MDA8) ozone and precursors carbon monoxide and nitrogen oxides for the summer of 2023. The lower Panel shows the daily (24 h) active fires obtained from MODIS satellite products at 1 km resolution (MOD13A1)†. Colored bars indicate confidence (high, nominal and low) based on infrared radiation emission. The map (left Panel) shows the active fires during February in central Chile.

https://doi.org/10.5194/egusphere-2024-328
Preprint. Discussion started: 12 February 2024
© Author(s) 2024. CC BY 4.0 License.

† We obtained information about active fires from the Terra Moderate Resolution Imaging Spectroradiometer (MODIS) Thermal Anomalies and Fire Daily (MOD14A1) satellite product (Giglio and Justice, 2021). The product includes a 1-km gridded fire mask providing information about the confidence level (low, nominal, or high) of fire activity possibly detected in each grid cell over the 24-hour compositing period. Using MOD14A1 grid cells within Chilean continental territory from 33ºS to 39ºS, we derived daily time series of the total number of pixels with active fires for each confidence level.

Data availability: Datasets used in this research are available in TOAR-II database.

Author contribution: RS, NR, TN, MC & YE: conceptualization; RS, LC & CO: methodology, LC, TN, MC & MG: data curation; RS, LC, CO & TC: formal analysis, RS: writing - original draft preparation; All authors: writing – review & editing.

Competing interest: The authors declare that they have no conflict of interest.

Special issue statement: This article is part of the special issue "Tropospheric Ozone Assessment Report Phase II (TOAR-II) Community Special Issue (ACP/AMT/BG/GMD inter-journal SI)". It is a result of the Tropospheric Ozone Assessment Report, Phase II (TOAR-II, 2020–2024).

Acknowledgments: This research was partially supported by ANID/FONDAP/1522A000; Powered@NLHPC: This research was partially supported by the supercomputing infrastructure of the NLHPC (ECM-02); We thank and acknowledge the use of data from the following public networks: Quito Air Quality Network, Secretariat of the Environment.

References

Adame, J. A., Cupeiro, M., Yela, M., Cuevas, E., and Carbajal, G.: Ozone and carbon monoxide at the Ushuaia GAW-WMO global station, Atmos Res, 217, https://doi.org/10.1016/j.atmosres.2018.10.015, 2019.

Andrade, M. de F., Kumar, P., de Freitas, E. D., Ynoue, R. Y., Martins, J., Martins, L. D., Nogueira, T., Perez-Martinez, P., de Miranda, R. M., Albuquerque, T., Gonçalves, F. L. T., Oyama, B., and Zhang, Y.: Air quality in the megacity of São Paulo: Evolution over the last 30 years and future perspectives, Atmos Environ, 159, 66–82, https://doi.org/https://doi.org/10.1016/j.atmosenv.2017.03.051, 2017.

Anet, G. J., Steinbacher, M., Gallardo, L., Velásquez Álvarez, A. P., Emmenegger, L., and Buchmann, B.: Surface ozone in the Southern Hemisphere: 20 years of data from a site with a unique setting in El Tololo, Chile, Atmos Chem Phys, 17, https://doi.org/10.5194/acp-17-6477-2017, 2017.

Ballesteros-González, K., Sullivan, A. P., and Morales-Betancourt, R.: Estimating the air quality and health impacts of biomass burning in northern South America using a chemical transport model, Science of the Total Environment, 739, https://doi.org/10.1016/j.scitotenv.2020.139755, 2020.

Carvalho, V. S. B., Freitas, E. D., Martins, L. D., Martins, J. A., Mazzoli, C. R., and Andrade, M. de F.: Air quality status and trends over the Metropolitan Area of São Paulo, Brazil as a result of emission control policies, Environ Sci Policy, 47, https://doi.org/10.1016/j.envsci.2014.11.001, 2015.

Cazorla, M. and Herrera, E.: Air quality in the Galapagos Islands: A baseline view from remote sensing and *in situ* measurements, Meteorological Applications, 27, https://doi.org/10.1002/met.1878, 2020.

Cazorla, M., Gallardo, L., and Jimenez, R.: The complex Andes region needs improved efforts to face climate extremes, Elementa, 10, https://doi.org/10.1525/elementa.2022.00092, 2022.

Cazorla, M., Herrera, E., Palomeque, E., and Saud, N.: What the COVID-19 lockdown revealed about photochemistry and ozone production in Quito, Ecuador, Atmos Pollut Res, 12, https://doi.org/10.1016/j.apr.2020.08.028, 2021b.

Cazorla, M., Parra, R., Herrera, E., and da Silva, F. R.: Characterizing ozone throughout the atmospheric column over the tropical Andes from in situ and remote sensing observations, Elementa, 9, https://doi.org/10.1525/elementa.2021.00019, 2021a.

Cazorla, M.: Ozone structure over the equatorial Andes from balloon-borne observations and zonal connection with two tropical sea level sites, J Atmos Chem, 74, https://doi.org/10.1007/s10874-016-9348-2, 2017.

Chang, K.-L., Schultz, M. G., Koren, G., and Selke, N.: Guidance note on best statistical practices for TOAR analyses, 2023. Available at https://igacproject.org/sites/default/files/2023-04/STAT_recommendations_TOAR_analyses_0.pdf

Cooper, O. R., Schultz, M. G., Schröder, S., Chang, K. L., Gaudel, A., Benítez, G. C., Cuevas, E., Fröhlich, M., Galbally, I. E., Molloy, S., Kubistin, D., Lu, X., McClure-Begley, A., Nédélec, P., O'Brien, J., Oltmans, S. J., Petropavlovskikh, I., Ries, L., Senik, I., Sjöberg, K., Solberg, S., Spain, G. T., Spangl, W., Steinbacher, M., Tarasick, D., Thouret, V., and Xu, X.: Multi-decadal surface ozone trends at globally distributed remote locations, Elementa, 8, https://doi.org/10.1525/elementa.420, 2020.

Daskalakis, N., Gallardo, L., Kanakidou, M., Nüß, J. R., Menares, C., Rondanelli, R., Thompson, A. M., and Vrekoussis, M.: Impact of biomass burning and stratospheric intrusions in the remote South Pacific Ocean troposphere, Atmos Chem Phys, 22, https://doi.org/10.5194/acp-22-4075-2022, 2022.

Falvey, M. and Garreaud, R. D.: Regional cooling in a warming world: Recent temperature trends in the southeast Pacific and along the west coast of subtropical South America (1979-2006), Journal of Geophysical Research Atmospheres, 114, https://doi.org/10.1029/2008JD010519, 2009.

Feron, S., Cordero, R. R., Damiani, A., Oyola, P., Ansari, T., Pedemonte, J. C., Wang, C., Ouyang, Z., and Gallo, V.: Compound climate-pollution extremes in Santiago de Chile, Sci Rep, 13, https://doi.org/10.1038/s41598-023-33890-w, 2023.

Fleming, Z. L., Doherty, R. M., Von Schneidemesser, E., Malley, C. S., Cooper, O. R., Pinto, J. P., Colette, A., Xu, X., Simpson, D., Schultz, M. G., Lefohn, A. S., Hamad, S., Moolla, R., Solberg, S., and Feng, Z.: Tropospheric Ozone Assessment Report: Present-day ozone distribution and trends relevant to human health, Elem Sci Anth, 6, 12, https://doi.org/10.1525/elementa.273, 2018.

https://doi.org/10.5194/egusphere-2024-328
Preprint. Discussion started: 12 February 2024
© Author(s) 2024. CC BY 4.0 License.

Garreaud, R. D., Boisier, J. P., Rondanelli, R., Montecinos, A., Sepúlveda, H. H., and Veloso-Aguila, D.: The Central Chile Mega Drought (2010–2018): A climate dynamics perspective, International Journal of Climatology, 40, https://doi.org/10.1002/joc.6219, 2020.

Garreaud, R. D., Vuille, M., Compagnucci, R., and Marengo, J.: Present-day South American climate, Palaeogeogr Palaeoclimatol Palaeoecol, 281, https://doi.org/10.1016/j.palaeo.2007.10.032, 2009.

Giglio, L. and Justice, C.: MODIS/Terra Thermal Anomalies/Fire Daily L3 Global 1km SIN Grid V061 [Data set]. NASA EOSDIS Land Processes Distributed Active Archive Center. Accessed 2024-01-12 from https://doi.org/10.5067/MODIS/MOD14A1.061

González-Reyes, Á., Jacques-Coper, M., Bravo, C., Rojas, M., and Garreaud, R.: Evolution of heatwaves in Chile since 1980, Weather Clim Extrem, 41, https://doi.org/10.1016/j.wace.2023.100588, 2023.

González, M. E., Gómez-González, S., Lara, A., Garreaud, R., and Díaz-Hormazábal, I.: The 2010–2015 Megadrought and its influence on the fire regime in central and south-central Chile, Ecosphere, 9, https://doi.org/10.1002/ecs2.2300, 2018.

Gu, G. and Adler, R. F.: Observed variability and trends in global precipitation during 1979–2020, Clim Dyn, 61, https://doi.org/10.1007/s00382-022-06567-9, 2023.

Gumbricht, T., Roman-Cuesta, R. M., Verchot, L., Herold, M., Wittmann, F., Householder, E., Herold, N., and Murdiyarso, D.: An expert system model for mapping tropical wetlands and peatlands reveals South America as the largest contributor, Glob Chang Biol, 23, https://doi.org/10.1111/gcb.13689, 2017.

Heinrich, V. H. A., Dalagnol, R., Cassol, H. L. G., Rosan, T. M., de Almeida, C. T., Silva Junior, C. H. L., Campanharo, W. A., House, J. I., Sitch, S., Hales, T. C., Adami, M., Anderson, L. O., and Aragão, L. E. O. C.: Large carbon sink potential of secondary forests in the Brazilian Amazon to mitigate climate change, Nat Commun, 12, https://doi.org/10.1038/s41467-021-22050-1, 2021.

Hoyos-Santillan, J., Miranda, A., Lara, A., Rojas, M., and Sepulveda-Jauregui, A.: Protecting Patagonian peatlands in Chile, https://doi.org/10.1126/science.aaz9244, 2019.

Jacques-Coper, M., Veloso-Aguila, D., Segura, C., and Valencia, A.: Intraseasonal teleconnections leading to heat waves in central Chile, International Journal of Climatology, https://doi.org/10.1002/joc.7096, 2021.

Juncosa Calahorrano, J. F., Lindaas, J., O'Dell, K., Palm, B. B., Peng, Q., Flocke, F., Pollack, I. B., Garofalo, L. A., Farmer, D. K., Pierce, J. R., Collett, J. L., Weinheimer, A., Campos, T., Hornbrook, R. S., Hall, S. R., Ullmann, K., Pothier, M. A., Apel, E. C., Permar, W., Hu, L., Hills, A. J., Montzka, D., Tyndall, G., Thornton, J. A., and Fischer, E. V.: Daytime Oxidized Reactive Nitrogen Partitioning in Western U.S. Wildfire Smoke Plumes, Journal of Geophysical Research: Atmospheres, 126, https://doi.org/10.1029/2020JD033484, 2021.

Kloss, C., Sellitto, P., von Hobe, M., Berthet, G., Smale, D., Krysztofiak, G., Xue, C., Qiu, C., Jégou, F., Ouerghemmi, I., and Legras, B.: Australian Fires 2019–2020: Tropospheric and Stratospheric Pollution Throughout the Whole Fire Season, Front Environ Sci, 9, https://doi.org/10.3389/fenvs.2021.652024, 2021.

https://doi.org/10.5194/egusphere-2024-328
Preprint. Discussion started: 12 February 2024
© Author(s) 2024. CC BY 4.0 License.

Lan, X., Thoning, K.W., and Dlugokencky, E.J.: Trends in globally-averaged CH_4, N_2O, and SF_6 determined from NOAA Global Monitoring Laboratory measurements. Version 2024-01, https://doi.org/10.15138/P8XG-AA10

Lapere, R., Huneeus, N., Mailler, S., Menut, L., and Couvidat, F.: Meteorological export and deposition fluxes of black carbon on glaciers of the central Chilean Andes, Atmos Chem Phys, 23, https://doi.org/10.5194/acp-23-1749-2023, 2023.

Lapere, R., Menut, L., Mailler, S., and Huneeus, N.: Seasonal variation in atmospheric pollutants transport in central Chile: Dynamics and consequences, Atmos Chem Phys, 21, https://doi.org/10.5194/acp-21-6431-2021, 2021.

Lu, X., Zhang, L., Zhao, Y., Jacob, D. J., Hu, Y., Hu, L., Gao, M., Liu, X., Petropavlovskikh, I., McClure-Begley, A., and Querel, R.: Surface and tropospheric ozone trends in the Southern Hemisphere since 1990: possible linkages to poleward expansion of the Hadley circulation, Sci Bull (Beijing), 64, https://doi.org/10.1016/j.scib.2018.12.021, 2019.

Lyu, X., Li, K., Guo, H., Morawska, L., Zhou, B., Zeren, Y., Jiang, F., Chen, C., Goldstein, A. H., Xu, X., Wang, T., Lu, X., Zhu, T., Querol, X., Chatani, S., Latif, M. T., Schuch, D., Sinha, V., Kumar, P., Mullins, B., Seguel, R., Shao, M., Xue, L., Wang, N., Chen, J., Gao, J., Chai, F., Simpson, I., Sinha, B., and Blake, D. R.: A synergistic ozone-climate control to address emerging ozone pollution challenges, https://doi.org/10.1016/j.oneear.2023.07.004, 2023.

Mena-Carrasco, M., Oliva, E., Saide, P., Spak, S. N., de la Maza, C., Osses, M., Tolvett, S., Campbell, J. E., Tsao, T. es C. C., and Molina, L. T.: Estimating the health benefits from natural gas use in transport and heating in Santiago, Chile, Science of the Total Environment, 429, https://doi.org/10.1016/j.scitotenv.2012.04.037, 2012.

Menares, C., Gallardo, L., Kanakidou, M., Seguel, R., and Huneeus, N.: Increasing trends (2001–2018) in photochemical activity and secondary aerosols in Santiago, Chile, Tellus B Chem Phys Meteorol, 72, https://doi.org/10.1080/16000889.2020.1821512, 2020.

Mendez-Espinosa, J. F., Belalcazar, L. C., and Morales Betancourt, R.: Regional air quality impact of northern South America biomass burning emissions, Atmos Environ, 203, https://doi.org/10.1016/j.atmosenv.2019.01.042, 2019.

Molina, L. T., Gallardo, L., Andrade, M., Baumgardner, D., Borbor-Cõrdova, M., Bõrquez, R., Casassa, G., Cereceda-Balic, F., Dawidowski, L., Garreaud, R., Huneeus, N., Lambert, F., McCarty, J. L., Mc Phee, J., Mena-Carrasco, M., Raga, G. B., Schmitt, C., and Schwarz, J. P.: Pollution and its Impacts on the South American Cryosphere, https://doi.org/10.1002/2015EF000311, 2015.

Muggeo, V. M. R.: Estimating regression models with unknown break-points, Stat Med, 22, https://doi.org/10.1002/sim.1545, 2003.

Nogueira, T., Kamigauti, L. Y., Pereira, G. M., Gavidia-Calderón, M. E., Ibarra-Espinosa, S., De Oliveira, G. L., De Miranda, R. M., De Castro Vasconcellos, P. D., De Freitas, E. D., and De Fatima Andrade, M.: Evolution of Vehicle Emission Factors in a Megacity Affected by Extensive Biofuel Use: Results of Tunnel Measurements in São Paulo, Brazil, Environ Sci Technol, 55, https://doi.org/10.1021/acs.est.1c01006, 2021.

Osses, M., Rojas, N., Ibarra, C., Valdebenito, V., Laengle, I., Pantoja, N., Osses, D., Basoa, K., Tolvett, S., Huneeus, N., Gallardo, L., and Gómez, B.: High-resolution spatial-distribution maps of road transport exhaust emissions in Chile, 1990-2020, Earth Syst Sci Data, 14, https://doi.org/10.5194/essd-14-1359-2022, 2022.

Pérez-Martínez, P. J., de Fátima Andrade, M., and de Miranda, R. M.: Traffic-related air quality trends in São Paulo, Brazil, J Geophys Res, 120, https://doi.org/10.1002/2014JD022812, 2015.

Population Reference Bureau: https://www.prb.org/international/geography/south-america/, last access: 30 January 2024.

Putero, D., Cristofanelli, P., Chang, K.-L., Dufour, G., Beachley, G., Couret, C., Effertz, P., Jaffe, D. A., Kubistin, D., Lynch, J., Petropavlovskikh, I., Puchalski, M., Sharac, T., Sive, B. C., Steinbacher, M., Torres, C., and Cooper, O. R.: Fingerprints of the COVID-19 economic downturn and recovery on ozone anomalies at high-elevation sites in North America and western Europe, Atmos Chem Phys, 23, 15693–15709, https://doi.org/10.5194/acp-23-15693-2023, 2023.

Rojas, N. Y., Mangones, S. C., Osses, M., Granier, C., Laengle, I., Alfonso A., J. V., and Mendez, J. A.: Road transport exhaust emissions in Colombia. 1990–2020 trends and spatial disaggregation, Transp Res D Transp Environ, 121, https://doi.org/10.1016/j.trd.2023.103780, 2023.

Schuch, D., de Freitas, E. D., Espinosa, S. I., Martins, L. D., Carvalho, V. S. B., Ramin, B. F., Silva, J. S., Martins, J. A., and de Fatima Andrade, M.: A two decades study on ozone variability and trend over the main urban areas of the São Paulo state, Brazil, Environmental Science and Pollution Research, 26, https://doi.org/10.1007/s11356-019-06200-z, 2019.

Schultz, M. G., Schröder, S., Lyapina, O., Cooper, O., Galbally, I., Petropavlovskikh, I., Von Schneidemesser, E., Tanimoto, H., Elshorbany, Y., Naja, M., Seguel, R., Dauert, U., Eckhardt, P., Feigenspahn, S., Fiebig, M., Hjellbrekke, A.-G., Hong, Y.-D., Christian Kjeld, P., Koide, H., Lear, G., Tarasick, D., Ueno, M., Wallasch, M., Baumgardner, D., Chuang, M.-T., Gillett, R., Lee, M., Molloy, S., Moolla, R., Wang, T., Sharps, K., Adame, J. A., Ancellet, G., Apadula, F., Artaxo, P., Barlasina, M., Bogucka, M., Bonasoni, P., Chang, L., Colomb, A., Cuevas, E., Cupeiro, M., Degorska, A., Ding, A., Fröhlich, M., Frolova, M., Gadhavi, H., Gheusi, F., Gilge, S., Gonzalez, M. Y., Gros, V., Hamad, S. H., Helmig, D., Henriques, D., Hermansen, O., Holla, R., Huber, J., Im, U., Jaffe, D. A., Komala, N., Kubistin, D., Lam, K.-S., Laurila, T., Lee, H., Levy, I., Mazzoleni, C., Mazzoleni, L., McClure-Begley, A., Mohamad, M., Murovic, M., Navarro-Comas, M., Nicodim, F., Parrish, D., Read, K. A., Reid, N., Ries, L., Saxena, P., Schwab, J. J., Scorgie, Y., Senik, I., Simmonds, P., Sinha, V., Skorokhod, A., Spain, G., Spangl, W., Spoor, R., Springston, S. R., Steer, K., Steinbacher, M., Suharguniyawan, E., Torre, P., Trickl, T., Weili, L., Weller, R., Xu, X., Xue, L., and Zhiqiang, M.: Tropospheric Ozone Assessment Report: Database and Metrics Data of Global Surface Ozone Observations, Elem Sci Anth, https://doi.org/10.1525/elementa.244, 2017.

Seguel, R. J., Gallardo, L., Fleming, Z. L., and Landeros, S.: Two decades of ozone standard exceedances in Santiago de Chile, Air Qual Atmos Health, 13, https://doi.org/10.1007/s11869-020-00822-w, 2020.

Seguel, R. J., Gallardo, L., Osses, M., Rojas, N. Y., Nogueira, T., Menares, C., de Fatima Andrade, M., Belalcázar, L. C., Carrasco, P., Eskes, H., Fleming, Z. L., Huneeus, N., Ibarra-Espinosa, S., Landulfo, E., Leiva, M., Mangones, S. C., Morais, F. G., Moreira, G. A., Pantoja, N., Parraguez, S., Rojas, J. P., Rondanelli, R., da Silva Andrade, I., Toro, R., and Yoshida, A. C.: Photochemical sensitivity to emissions and local meteorology in Bogotá, Santiago, and São Paulo, Elementa: Science of the Anthropocene, 10, https://doi.org/10.1525/elementa.2021.00044, 2022.

https://doi.org/10.5194/egusphere-2024-328
Preprint. Discussion started: 12 February 2024
© Author(s) 2024. CC BY 4.0 License.

Seguel, R. J., Garreaud, R., Muñoz, R., Bozkurt, D., Gallardo, L., Opazo, C., Jorquera, H., Castillo, L., and Menares, C.: Volatile organic compounds measured by proton transfer reaction mass spectrometry over the complex terrain of Quintero Bay, Central Chile, Environmental Pollution, 330, https://doi.org/10.1016/j.envpol.2023.121759, 2023.

Seguel, R. J., Mancilla, C. A., Rondanelli, R., Leiva, M. A., and Morales, R. G. E.: Ozone distribution in the lower troposphere over complex terrain in Central Chile, Journal of Geophysical Research Atmospheres, 118, https://doi.org/10.1002/jgrd.50293, 2013.

Silva Júnior, R. S. da, Oliveira, M. G. L. de, and Andrade, M. de F.: Weekend/weekday differences in concentrations of ozone, nox, and non-methane hydrocarbon in the metropolitan area of São Paulo, Revista Brasileira de Meteorologia, 24, https://doi.org/10.1590/s0102-77862009000100010, 2009.

Silva, J. S., Rojas, J. P., Norabuena, M., and Seguel, R. J.: Ozone and volatile organic compounds in the metropolitan area of Lima-Callao, Peru, Air Qual Atmos Health, https://doi.org/10.1007/s11869-018-0604-2, 2018.

Sokhi, R. S., Singh, V., Querol, X., Finardi, S., Targino, A. C., Andrade, M. de F., Pavlovic, R., Garland, R. M., Massagué, J., Kong, S., Baklanov, A., Ren, L., Tarasova, O., Carmichael, G., Peuch, V. H., Anand, V., Arbilla, G., Badali, K., Beig, G., Belalcazar, L. C., Bolignano, A., Brimblecombe, P., Camacho, P., Casallas, A., Charland, J. P., Choi, J., Chourdakis, E., Coll, I., Collins, M., Cyrys, J., da Silva, C. M., Di Giosa, A. D., Di Leo, A., Ferro, C., Gavidia-Calderon, M., Gayen, A., Ginzburg, A., Godefroy, F., Gonzalez, Y. A., Guevara-Luna, M., Haque, S. M., Havenga, H., Herod, D., Hõrrak, U., Hussein, T., Ibarra, S., Jaimes, M., Kaasik, M., Khaiwal, R., Kim, J., Kousa, A., Kukkonen, J., Kulmala, M., Kuula, J., La Violette, N., Lanzani, G., Liu, X., MacDougall, S., Manseau, P. M., Marchegiani, G., McDonald, B., Mishra, S. V., Molina, L. T., Mooibroek, D., Mor, S., Moussiopoulos, N., Murena, F., Niemi, J. V., Noe, S., Nogueira, T., Norman, M., Pérez-Camaño, J. L., Petäjä, T., Piketh, S., Rathod, A., Reid, K., Retama, A., Rivera, O., Rojas, N. Y., Rojas-Quincho, J. P., San José, R., Sánchez, O., Seguel, R. J., Sillanpää, S., Su, Y., Tapper, N., Terrazas, A., Timonen, H., Toscano, D., Tsegas, G., Velders, G. J. M., Vlachokostas, C., von Schneidemesser, E., VPM, R., Yadav, R., Zalakeviciute, R., and Zavala, M.: A global observational analysis to understand changes in air quality during exceptionally low anthropogenic emission conditions, Environ Int, 157, https://doi.org/10.1016/j.envint.2021.106818, 2021.

Squizzato, R., Nogueira, T., Martins, L. D., Martins, J. A., Astolfo, R., Machado, C. B., Andrade, M. de F., and Freitas, E. D. de: Beyond megacities: tracking air pollution from urban areas and biomass burning in Brazil, NPJ Clim Atmos Sci, 4, https://doi.org/10.1038/s41612-021-00173-y, 2021.

Szopa, S., Naik, V., Adhikary, B., Artaxo, P., Berntsen, T., Collins, W.D., Fuzzi, S., Gallardo, L., Kiendler-Scharr, A., Klimont, Z., Liao, H., Unger, N., and Zanis, P.: Short-Lived Climate Forcers. In *Climate Change 2021: The Physical Science Basis. Contribution of Working Group I to the Sixth Assessment Report of the Intergovernmental Panel on Climate Change* [Masson-Delmotte, V., P. Zhai, A. Pirani, S.L. Connors, C. Péan, S. Berger, N. Caud, Y. Chen, L. Goldfarb, M.I. Gomis, M. Huang, K. Leitzell, E. Lonnoy, J.B.R. Matthews, T.K. Maycock, T. Waterfield, O. Yelekçi, R. Yu, and B. Zhou (eds.)]. Cambridge University Press, Cambridge, United Kingdom and New York, NY, USA, pp. 817–922, doi:10.1017/9781009157896.008, 2021

© Author(s) 2024. CC BY 4.0 License.

Tarasick, D., Galbally, I. E., Cooper, O. R., Schultz, M. G., Ancellet, G., Leblanc, T., Wallington, T. J., Ziemke, J., Liu, X., Steinbacher, M., Staehelin, J., Vigouroux, C., Hannigan, J. W., García, O., Foret, G., Zanis, P., Weatherhead, E., Petropavlovskikh, I., Worden, H., Osman, M., Liu, J., Chang, K. L., Gaudel, A., Lin, M., Granados-Muñoz, M., Thompson, A. M., Oltmans, S. J., Cuesta, J., Dufour, G., Thouret, V., Hassler, B., Trickl, T., and Neu, J. L.: Tropospheric ozone assessment report: Tropospheric ozone from 1877 to 2016, observed levels, trends and uncertainties, https://doi.org/10.1525/elementa.376, 2019.

Valverde, M. C. and Rosa, M. B.: Heat waves in São Paulo State, Brazil: Intensity, duration, spatial scope, and atmospheric characteristics, International Journal of Climatology, 43, https://doi.org/10.1002/joc.8058, 2023.